Characterization of Mechanical and Corrosion Properties of Mo-free Low Alloy Steels for Secondary Pipeline Application

Seunghyun Kim[1], Gidong Kim[1,2], and Ji Hyun Kim[1*]

[1] *Department of Nuclear Engineering, School of Mechanical, Aerospace and Nuclear Engineering, Ulsan National Institute of Science and Technology (UNIST)*
[2] *Joining Technology Department, Korea Institute of Materials Science (KIMS)*
*kimjh@unist.ac.kr

1. Introduction

Degradation of pipeline materials in secondary system of nuclear power plants has many forms such as flow-accelerated corrosion, cavitation-erosion, liquid drop impingement erosion, etc. Due to these flow-induced materials degradation (FIMD), catastrophic failure of pipelines occurred in the operating history of nuclear power plants such as Surry Unit-3 accident [1, 2]. Therefore, many countermeasures to mitigate FIMD have been employed since the corrosion rate of carbon steel pipelines is very sensitive to water and alloy chemistries.

In terms of water chemistry, pH, dissolved oxygen concentration, temperature, etc. are known as key parameters to determine the corrosion rate of carbon steels [3, 4]. When it comes to alloy chemistry, chemical composition of Cr, Mo, and Cu is known as to dominate the corrosion rate [5]. However, while the role of Cr is relatively well known, that of Mo is not clearly investigated especially in high-temperature flowing water environments. And, according to the Ducreux's FAC rate equation, it is possible to substitute Mo with Cr. Since the total length of pipelines in secondary system of pressurized water reactor is more than 100 km, it is very cost-effective for construction and maintenance of the power plants because Mo is far more expensive than Fe and Cr.

In this study, we manufactured 3 different low alloy steels with different Cr and Mo contents – Fe-2.25Cr-1Mo-0.1C, Fe-3.2Cr-0.5Mo-0.1C, and Fe-4.2Cr-0.1C by employing vacuum arc remelting (VAR) methods. And, their mechanical properties and corrosion characteristics were evaluated. Their performance in high-temperature flowing water will be evaluated as well.

2. Materials and Methods

2.1. Manufacturing of the Alloys

Chemical composition of the alloys is determined by Decreux's FAC rate equation as follows.

$$FAC\ Rate = 1/(83[Cr]^{0.89}[Cu]^{0.25}[Mo]^{0.2}) \qquad (1)$$

Where FAC rate is the relative FAC, and [Cr], [Cu], [Mo] are chemical composition in wt.%. Table 1 enlists the chemical composition of the manufactured alloys.

Sample 1 has same Cr and Mo composition with ASTM A335 P22, which is currently used low alloy steel for commercial pressurized water reactors. Sample 2 possesses higher Cr but lower Mo composition. And, Sample 3 possesses no Mo, as Mo-free alloy with same FAC rate to Sample 1.

Table 1. Chemical composition and Decreux's FAC rate of the manufactured alloys

	[Cr] (wt.%)	**[Mo] (wt.%)**	**[C] (wt.%)**	**Decreux's FAC Rate (vs. P22)**
Sample 1	2.25	1	0.1	1
Sample 2	3.2	0.5	0.1	0.840
Sample 3	4.2	0	0.1	1.045

For manufacturing of the alloys, VAR methods was employed. In vacuum environments, feedstock materials (>99.9 % Fe, Cr, Mo, and C) were prepared, and plasma arc melted the feedstock materials. After furnace cooling, the manufactured ingots had a size of 100 mm in diameter and 15 mm in thickness (Figure 1d). Then the ingots were hot rolled until the thickness reaches less than 3 mm and air cooled. The hot rolled ingots finally normalized and tempered in 970 °C for 30 min and 675 °C for 10 min, respectively. After the normalizing and the tempering, the ingots were air cooled.

2.2. Characterization of Mechanical Properties

The tension testing and the hardness measurement were conducted for the manufactured ingots. For the tension testing, the plate-type specimens were prepared according to ASTM E8/E8M – 16a. Strain rate was set to 0.3375 mm/min. For the hardness measurements, 10 point were in the center region of the specimens based on Vickers hardness.

2.3. Corrosion Tests

For the characterization of corrosion properties, electrochemical impedance spectroscopy (EIS) and linear sweep voltammetry (LSV) were employed in 3.5 wt. % NaCl solution. EIS measurements were conducted with 0 V DC potential, 10 mV AC amplitude from 10^{-2} to 10^6 Hz frequency domain. LSV were conducted with -0.2 to 2.5 V potential range. The test sequence was stabilization of open circuit potential – EIS – LSV.

After the second EIS measurements, microstructure of the surfaces were observed by optical microscopy.

3. Results and Discussion

2.1. Microstructure

The microstructures of the manufactured alloys are displayed in Figure 2. Figure 2a shows a mixture of ferrite and cementite. And, typical microstructure of P22, which is normalized and tempered, is bainite and this well matches with the microstructure of sample 1. Sample 2 also shows bainite structure likewise to sample 1 (Figure 2b). However, composition of ferrite decreases as contents of Mo decreases. In case of sample 3 (Figure 2c), bainite structure is observable but ferrite is barely visible.

Table 2. Results of Vickers hardness tests (10 points averaged) and tension testing for the manufactured samples

Sample	Hardness (HV)	Yield Strength (MPa)	Tensile Strength (MPa)
Sample 1	211±7.07	270.4	356.6
Sample 2	208±5.88	372.4	462.8
Sample 3	183±3.95	350.2	446.4

2.2. Characterization of Mechanical Properties

The results of measured hardness and tension testings are enlisted in **Table 2**. Hardness requirements for ASTM A335 P22 is maximum 265 HV?? [6]. Thus, all the samples meet the hardness requirements. There is a tendency that as Mo decreases, the hardness decreases.

Table 2 also shows the relationship between stress and elongation for the manufactured alloys. Yield and tensile strength of sample 1 is 270.4 and 356.6 MPa, respectively. For sample 2, yield and tensile strength values are 372.4 and 462.8 MPa. For sample 3, those values are 350.2 and 446.4 MPa. It is observed that the yield and the tensile strength of sample 1 are far less than samples 2 and 3.

2.3. Corrosion Tests

The results from EIS, which were measured in 3.5 wt.% NaCl solution after the stabilization of open circuit potential, are displayed in Figure 3. The fitting of the EIS was conducted using Randle's circuit model, which is generally used for the corrosion of metallic specimen
.
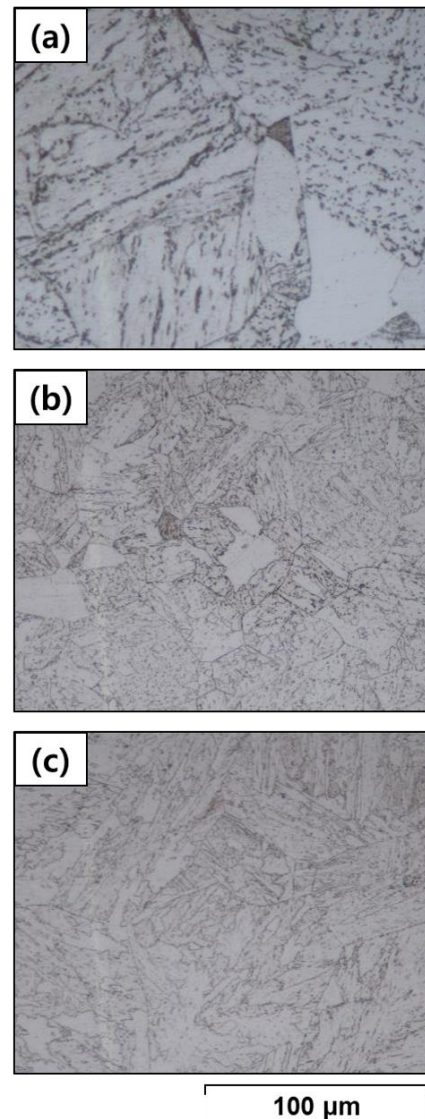
Figure 2. Microstructures of (a) Sample 1, (b) Sample 2, and (c) Sample 3.
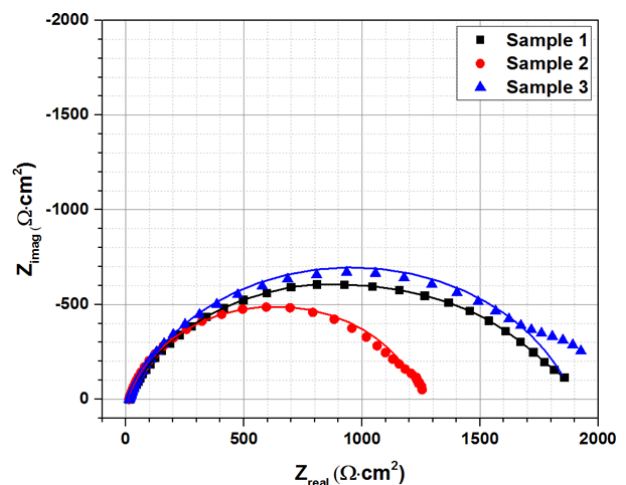
Figure 3. Nyquist plots of the manufactured alloys with fit results (solid lines) in 3.5 wt.% NaCl solution

The EIS results show that the ohmic resistance of samples 1 and 3 is similar with 1797 and 1881 $\Omega \cdot cm^2$, respectively. Furthermore, double layer capacitance of sample 2 is 97.4 $\mu F/cm^2$, indicating that permittivity of the double layer.
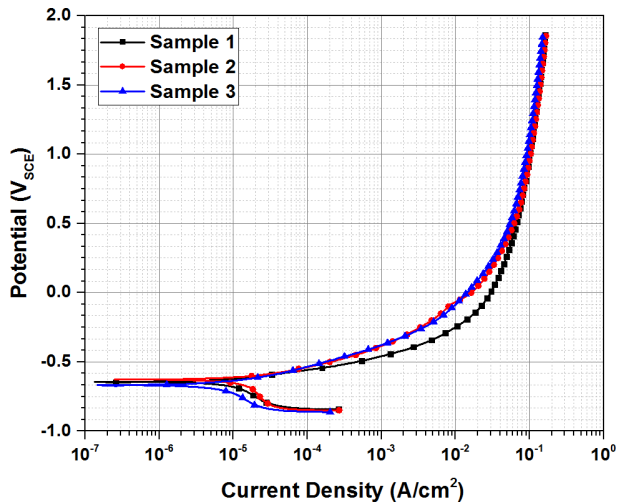
Figure 4. LSV results of the manufactured alloys in 3.5 wt.% NaCl solution

Figure 4 indicate the LSV results of the manufactured alloys. All the samples represent similar equilibrium potential values. However, sample 2 has the highest exchange current density values, 9.16 $\mu A/cm^2$, and the that of sample 3 is lowest, 6.58 $\mu A/cm^2$. This indicates that the corrosion resistance of sample 3 in 3.5 wt.% NaCl solution is better than the others. Also, pitting of the samples was not observable.

4. Conclusion

For the mitigation of FIMD in secondary system of nuclear power plants in cost-effective way, we have developed Mo-free low alloy steels (Fe-4.2Cr) as a substitution for ASTM A335, which contains 2.25Cr-1Mo. By employing VAR methods, the alloys were successfully manufactured followed by hot-rolling, normalizing in 975 °C, and tempering in 675 °C. Prior to high-temperature corrosion tests, their mechanical and electrochemical properties were tested using Vickers hardness measurements, tension testing, EIS and LSV. The hardness and the tension testing shows that the samples meet the requirements of ASTM A335. Corrosion tests also show that their performance is comparable or even better than ASTM A335. As future works, their performance in high-temperature flowing water will be experimentally demonstrated.

5. Acknowledgements

REFERENCES

1. Trevin, S., *7 - Flow accelerated corrosion (FAC) in nuclear power plant components*, in *Nuclear Corrosion Science and Engineering*, D. Féron, Editor. 2012, Woodhead Publishing. p. 186-229.
2. Chexal, B., J. Horowitz, and B. Dooley, *Flow-accelerated corrosion in power plants. Revision 1*. 1998, ; Electric Power Research Inst., Palo Alto, CA (United States);Electricite de France (France);Siemens AG Power Generation (Germany). p. Medium: X; Size: [300] p.
3. Fujiwara, K., et al., *Model of physico-chemical effect on flow accelerated corrosion in power plant.* Corrosion Science, 2011. **53**(11): p. 3526-3533.
4. Fujiwara, K., et al., *Correlation of flow accelerated corrosion rate with iron solubility.* Nuclear Engineering and Design, 2011. **241**(11): p. 4482-4486.
5. Munson, A.M.D., *Flow-Accelerated Corrosion Investigation of Trace Chromium*. 2003, EPRI: Palo Alto, CA.
6. Wu, P.C., *Erosion/Corrosion-induced Pipe Wall Thinning in U.S. Nuclear Power Plants*, P.C. Wu, Editor. 1989, U.S. Nuclear Regulatory Comission: Washington, DC 20555.